

## Design of Electrochromic Asymmetric Multilayered Structure for Smart Windows

Xueyu Wang

State Key Laboratory of Information Photonics and Optical  
Communications  
Beijing University of Posts and Telecommunications  
Beijing, China  
xueyuwang@bupt.edu.cn

Yumin Liu

State Key Laboratory of Information Photonics and Optical  
Communications  
Beijing University of Posts and Telecommunications  
Beijing, China  
microliuyumin@hotmail.com

**Abstract**—Smart windows can moderate the transmission and absorption of sunlight according to seasonal changes and personal preferences. Here, we designed a multilayer thin-film structure of an electrochromic smart window that can effectively regulate the transmission and absorption by rotating the sample and adjusting the bias voltage. This lithography-free, polarization-independent, incident angle-insensitive structure with an extensive modulation transmission range improves new ideas for the future development of electrochromic windows.

**Keywords**—smart windows; thin-film; electrochromic

### I. INTRODUCTION

In recent decades, global warming and the energy crisis have been gaining attention. Building energy consumption accounts for 40-50% of global energy consumption, such as heating, cooling, and ventilation. Compared to conventional windows, smart windows can dynamically modulate the absorption, reflection, or transmission spectrum of solar energy according to individual preferences to reduce energy consumption [1]. Smart windows are usually designed for energy saving in the solar range (0.3 - 2.5  $\mu\text{m}$ ) and atmospheric transparent window range (8 - 13  $\mu\text{m}$ ) for reducing energy consumption. The use of daytime radiation cooling is capable of zero absorption in the solar band and high radiation in the atmospheric window range to achieve device temperatures lower than the surrounding temperature, which can be used to cool buildings and the human body. However, the ideal radiation cooling device's low efficiency and preparation complexity make it difficult to apply in practice. The solar spectrum, which contains a lot of energy, leaves more room for manipulation. There are four main types of smart windows working in the solar wavelength: electrochromic [2], mechanically induced opacity [3], photochromic, and thermochromic [4] windows. Electrochromic can change the material's refractive index by regulating the bias voltage according to personal preference, thus controlling the propagation direction and intensity of the sunlight, which has received much attention. Recently, Ma et al. designed a solar thermal asymmetric metasurface with a maximum 25% difference in absorption from different sides [5]. Chowdhary et al. proposed electrochromic smart window glasses using noble metals that can dynamically control the intensity of transmitted solar radiation, depending upon the weather/climate condition [6]. However, smart windows based on asymmetric structures with electrochromic are hardly reported.

To bridge the gap in the literature, we propose and numerically investigate a novel electrochromic asymmetric multilayered PMMA/Ag/DAST/Fe/substrate structure. It can change the direction of the incidence of electromagnetic waves by rotating the sample to realize the regulation of sunlight. In addition, bias voltage in two metal layers can change the refractive index of DAST and modify the Fabry-Perot cavity to admit the sunlight modulation further. When the bias voltage is 0, the absorption of the smart window from the front and back sides are 16.5% and 34.1%, respectively, and the transmittance is 62%. By the rotating sample and bias voltage (-15 - +15V), the weighted solar absorption of the smart window has a large adjustable range: 14-17% and 22-42%, and the transmittance range is 41-62%. This electrochromic, lithography-free, and simple multilayer film structure paves the way for the future development of smart windows for icephobicity, counteracting fogging, heat preservation building, etc.

### II. MODEL STRUCTURE AND CALCULATION METHOD

Figure 1(a) shows the schematic illustration of the potential application of metasurface for smart windows. In summer, the outside temperature is high, and the sunlight is strong, so only part of the visible light transmission is needed, while most of the sunlight is reflected. In this case, the indoor temperature is avoided from rising while ensuring sufficient light in the room. In the cold winter, the glass can be rotated 180° to minimize reflected sunlight, which can be used to maintain the room temperature or to heat the glass windows. In addition, the smart window has more space to regulate the reflection and transmission of sunlight under the effect of bias voltage.

The transmission matrix method (TMM) is used for multilayer thin-film systems to calculate the reflection, transmission, and absorption. The interaction between each layer of the film and the electromagnetic waves can be represented by a characteristic matrix ( $M_j$ ). The characteristic matrix of the  $j$  layer is:

$$M_j = \begin{bmatrix} \cos\delta_j & \frac{i\sin\delta_j}{\eta_j} \\ i\eta_j\sin\delta_j & \cos\delta_j \end{bmatrix} \quad (1)$$

where  $\delta_j = 2\pi n_j d_j \cos\theta_j / \lambda$ ,  $\eta_j = n_j \sqrt{\epsilon_0 / \mu_0} \cos\theta_j$  (TE-polarization), and  $\eta_j = n_j \sqrt{\epsilon_0 / \mu_0} / \cos\theta_j$  (TM-polarization),  $\lambda$  is the wavelength,

$d_j$ ,  $n_j$ , and  $\theta_j$  are the thickness, refractive index, and propagation angle of the  $j$ -layer medium.  $\epsilon_0$  and  $\mu_0$  are the vacuum permittivity and magnetism. The characteristic matrix [7,8] of the  $N$ -layer structure is:

$$M = \prod_{j=1}^N M_j = \begin{bmatrix} m_{11} & m_{12} \\ m_{21} & m_{22} \end{bmatrix} \quad (2)$$

The reflection and transmission coefficients of the structure are:

$$r = \frac{\eta_0 m_{11} + \eta_t m_{12} - m_{21} - \eta_t m_{22}}{\eta_0 m_{11} + \eta_0 \eta_t m_{12} + m_{21} + \eta_t m_{22}} \quad (3)$$

$$t = \frac{2\eta_0}{\eta_0 m_{11} + \eta_0 \eta_t m_{12} + m_{21} + \eta_t m_{22}} \quad (4)$$

where  $\eta_0$  and  $\eta_t$  are the modified admittance of the input port and the outgoing port of electromagnetic wave, respectively. Therefore, the reflection and transmittance can be represented as  $R = |r|^2$  and  $T = |t|^2$ , respectively. The absorption can be calculated as  $A = 1 - R - T$ . solar modulation ability ( $\Delta A_{\text{sol}}$ ), integral luminous transmittance ( $T_{\text{lum}}$ ) can be expressed as:

$$\Delta A_{\text{sol}} = \left| \frac{\int \Phi_{\text{sol}}(\lambda) A_{\text{front}}(\lambda) d\lambda}{\int \Phi_{\text{sol}}(\lambda) d\lambda} - \frac{\int \Phi_{\text{sol}}(\lambda) A_{\text{back}}(\lambda) d\lambda}{\int \Phi_{\text{sol}}(\lambda) d\lambda} \right| \quad (5)$$

$$T_{\text{lum}} = \frac{\int \Phi_{\text{lum}}(\lambda) T(\lambda) d\lambda}{\int \Phi_{\text{lum}}(\lambda) d\lambda} \quad (6)$$

where the  $A_{\text{front}}(\lambda)$  and  $A_{\text{back}}(\lambda)$  are the absorption spectrum of structure when light is incident on the front and back sides, respectively,  $\Phi_{\text{sol}}(\lambda)$  is the solar irradiance spectrum for an air mass of 1.5,  $\Phi_{\text{lum}}(\lambda)$  is the visibility function of the human eyes [9]. The refractive index of metals and  $\text{SiO}_2$  are taken from experimental data [10].

### III. RESULTS AND DISCUSSION

As shown in Fig. 1(b), the Ag, DAST, and Fe are placed on a thin  $\text{SiO}_2$  substrate, and the thickness of  $\text{SiO}_2$  is set to 500 nm. In the schematic, a 50 nm PMMA is covered on the structure, which can avoid metal oxidation and reduce reflection. PMMA with a low refractive index, low price, easy-to-fabricate, and high stability is frequently applied in optical design. The thickness of Ag, DAST, and Fe are indicated by  $d_{\text{Ag}}$ ,  $d_{\text{DAST}}$ , and  $d_{\text{Fe}}$ , and the  $d_{\text{Ag}}$ ,  $d_{\text{DAST}}$ , and  $d_{\text{Fe}}$ , are set to 12 nm, 60 nm, and 3 nm. There is a bias voltage between Ag and Fe metals. Fig. 2(a) and (b) plot the ideal transmission and ideal front and back absorption for electrochromic smart windows. Under this ideal condition,  $\Delta A_{\text{sol}}$  and  $T_{\text{lum}}$  can reach the maximum value. The light cyan color is the solar spectrum, and the light purple curve is the human eye visualization function. The green curve in Fig. 2(c) shows the transmission spectrum of the structure and the  $T_{\text{lum}} = 62\%$ . The inset shows the position of the sunlight transmission spectrum on the color coordinates, and the Ra of transmission is equal to 90. It is clear that the designed structure has high transmittance in the visible range and transmits sunlight in white color, which is very favorable for applications in architectural glass. Fig. 2(d)

illustrates the front and back irradiation absorption spectra. The  $A_{\text{front}}$  and  $A_{\text{back}}$  represent the weighted absorption for the front and back sides. The calculated  $A_{\text{front}}$  and  $A_{\text{back}}$  are 16.5% and 34.1%, and the calculated  $\Delta A_{\text{sol}}$  is 17.6%. In this case, smart windows can block most sunlight in summer, reduce the loss of sunlight in winter, and maintain high transmittance in the visible range and high Ra.

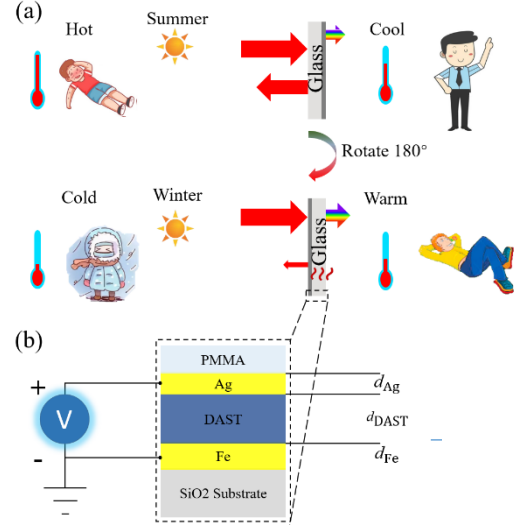


Figure 1. (a) The working principle diagram of smart windows in different seasons. (b) 2D schematic diagram of electrochromic metasurface with bias voltage supply.

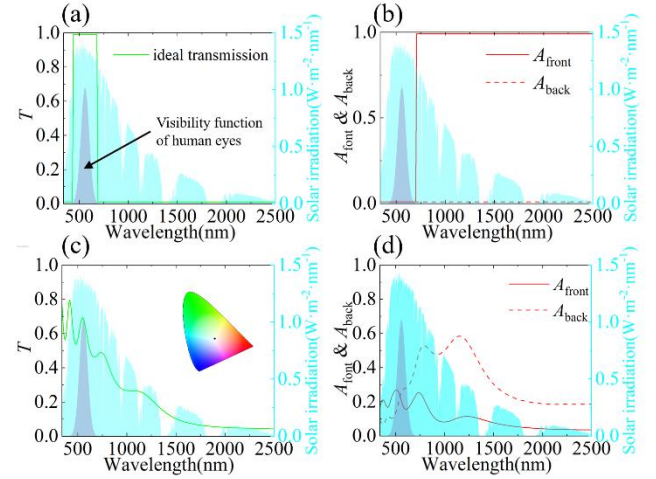


Figure 2. (a) ideal transmission and (b) ideal front and back absorption for electrochromic smart windows. (c) Transmission of the structure of metasurface. (d) The front and back irradiation absorption spectrum.

The DAST is an electro-optic polymer with a large electro-optic coefficient (3.41 nm/V), and it can achieve maximum tunability with minimum bias voltage. The refractive index of the DAST as a function of the applied voltage is given by [11]:

$$n_{\text{DAST}} = n_0 + \frac{dn}{du} \frac{V}{d_{\text{DAST}}} \quad (6)$$

Where  $n_0=2.2$  is the refractive index of the DAST polymer at zero bias voltage.  $\frac{dn}{du}=3.41$  nm/V is the electro-optic coefficient,  $u$  is the applied electric field, and  $V$  is the applied voltage. The  $d_{\text{DAST}}$  is the thickness of the DAST polymer. Fig. 3(a) shows the relationship between  $A_{\text{front}}$ ,  $A_{\text{back}}$ ,  $T_{\text{lum}}$ , and the bias voltage. The bias voltage variation in the -15 - +15V range, and  $d_{\text{Ag}}=13$  nm,  $d_{\text{DAST}}=60$  nm,  $d_{\text{Fe}}=3$  nm. It can be found that there is a wide range of variation in  $T_{\text{lum}}$  (41 - 62%). The  $A_{\text{back}}$  has a greater range of variation than the  $A_{\text{front}}$  when the voltage varies from -15 to +15V, and the range of  $A_{\text{front}}$  and  $A_{\text{back}}$  variation is in 14 - 17% and 22 - 42% ranges. In the summer heat, the bias voltage can be set to +15V, 33% of the sunlight's energy can be reflected, and the temperature of the building can be lowered. In the cold winter, the bias voltage can be set to -3 V. When the PMMA faces inside the building, the  $T_{\text{lum}}$  is 61%, and only 2% of the energy is reflected, which greatly maintains the indoor temperature. The energy absorbed by the smart window can be used for icephobicity and counteracting fogging. In addition, the absorption and transmission spectra of the smart window can be modulated according to personal preference by adjusting the bias voltage. Fig. 3(b) illustrates the CIE color coordinate position variation with the bias voltage. The transmitted sunlight has a high color rendering index when the bias voltage varies from -15 to +15V. The bias voltage does not change the color of the transmitted light of the glass, which keeps the comfort of human eyes and increases the practicality of smart windows.

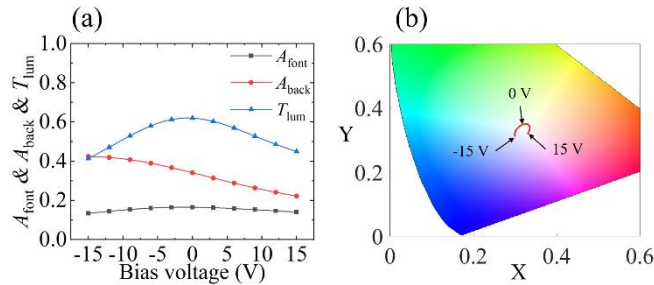


Figure 3. (a) The  $A_{\text{front}}$ ,  $A_{\text{back}}$  and  $T_{\text{lum}}$  as a function of bias voltage. (b) The position in CIE coordinates versus bias voltage.

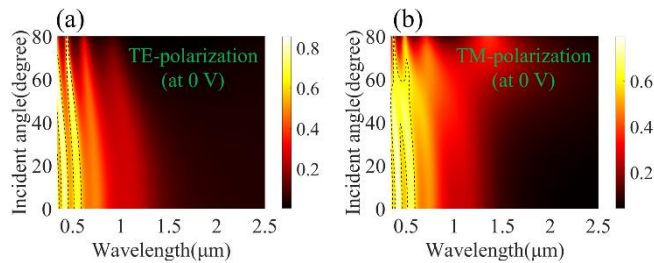


Figure 4. The light transmission spectrum versus the angle of incidence for different polarization conditions with the bias voltage of 0 V. (a) TE-polarization, (b) TM-polarization. The black dashed line represents the transmittance of 60%.

The smart window's transmission performance at oblique incidence is also analyzed to improve its practicality. Fig. 4(a) and (b) demonstrate the transmission characteristics of the smart window under TE and TM-polarized incident light as a

function of the angle of incidence. It can be seen that the structure maintains high transmission performance in the visible range even with an incidence angle larger than 60° for TE and TM-polarization. The transmittance of TM polarization is higher than that of TE polarization for the same incident angle.

#### IV. CONCLUSION

We propose a multilayer thin film structure for electrochromic windows. It can regulate the transmission and absorption of sunlight according to seasonal changes and personal preferences by rotating the sample and regulating the bias voltage. The bias voltage is between -15 - +15V, it can vary between 41-62% for  $T_{\text{lum}}$ , and the absorption of the glass can vary between 14 - 17% and 22 - 42%. This simple, polarization-independent, incident-angle-insensitive, multilayer film structure with a large modulated transmission range raises new possibilities for the future development of electrochromic windows.

#### ACKNOWLEDGMENT

This research was funded by the National Natural Science Foundation of China (NSFC) (61875021); Natural Science Foundation of Beijing (2192036); The Fundamental Research Funds for the Central Universities; Guangxi Key Laboratory of Wireless Wideband Communication and Signal Processing; BUPT Action Plan Project (ZDYY202102-1).

#### REFERENCES

- [1] S. Nundy, A. Mesloub, B. M. Alsolami, and A. Ghosh, "Electrically actuated visible and near-infrared regulating switchable smart window for energy positive building: A review," *Journal of Cleaner Production*, vol. 301, pp. 126854, 2021.
- [2] S. Zhang, S. Cao, T. Zhang, and J. Y. Lee, "Plasmonic Oxygen-Deficient TiO<sub>2</sub>-x Nanocrystals for Dual-Band Electrochromic Smart Windows with Efficient Energy Recycling," *Advanced materials*, vol. 32, no. 43, pp. 2004686, 2020.
- [3] Y. Ke, J. Chen, G. Lin, S. Wang, Y. Zhou, J. Yin, P. S. Lee, and Y. Long, "Smart Windows: Electro-, Thermo-, Mechano-, Photochromics, and Beyond," *Advanced Energy Materials*, vol. 9, no. 39, pp. 1902066, 2019.
- [4] M. Guo, Q. Yu, X. Wang, W. Xu, Y. Wei, Y. Ma, J. Yu, and B. Ding, "Tailoring Broad-Band-Absorbed Thermoplasmonic 1D Nanochains for Smart Windows with Adaptive Solar Modulation," *ACS Applied Materials & Interfaces*, vol. 13, no. 4, pp. 5634-5644, 2021.
- [5] R. Ma, D. Wu, Y. Liu, H. Ye, and D. Sutherland, "Copper plasmonic metamaterial glazing for directional thermal energy management," *Materials & Design*, vol. 188, pp. 108407, 2020.
- [6] A. K. Chowdhary and D. Sikdar, "Design of electro-tunable all-weather smart windows," *Solar Energy Materials and Solar Cells*, vol. 222, pp. 110921, 2021.
- [7] E.-T. Hu, X.-X. Liu, Y. Yao, K.-Y. Zang, Z.-J. Tu, A.-Q. Jiang, K.-H. Yu, J.-J. Zheng, W. Wei, Y.-X. Zheng, R.-J. Zhang, S.-Y. Wang, H.-B. Zhao, O. Yoshie, Y.-P. Lee, C.-Z. Wang, D. W. Lynch, J.-P. Guo, and L.-Y. Chen, "Multilayered metal-dielectric film structure for highly efficient solar selective absorption," *Materials Research Express*, vol. 5, no. 6, pp. 66428, 2018.
- [8] C. C. Katsidis and D. I. Siapkas, "General transfer-matrix method for optical multilayer systems with coherent, partially coherent, and incoherent interference," *Applied optics*, vol. 41, no. 19, pp. 3978-3987, 2002.
- [9] M. A. Green, "Limiting photovoltaic efficiency under new ASTM International G173-based reference spectra," *Progress in*

*Photovoltaics: Research and Applications*, vol. 20, no. 8, pp. 954–959, 2012.

- [10] E. D. Palik, “Handbook of optical constants of solids,” Academic press, 1998.
- [11] M. Aalizadeh, A. E. Serebryannikov, A. Khavasi, G. A. E. Vandenbosch, and E. Ozbay, “Toward electrically tunable, lithography-free, ultra-thin color filters covering the whole visible spectrum,” *Scientific reports*, vol. 8 no. 1, pp. 1-11, 2018.